AAC Journals.ASM.org

Preclinical Experiments on the Release Behavior of Biodegradable Nanofibrous Multipharmaceutical Membranes in a Model of Four-Wall Intrabony Defect

Dave Wei-Chih Chen,[a,b] Fu-Ying Lee,[c] Jun-Yi Liao,[d] Shih-Jung Liu,[b] Chao-Ying Hsiao,[b] Jan-Kan Chen[e]

Department of Orthopedic Surgery, Chang Gung Memorial Hospital, Kwei-Shan, Tao-Yuan, Taiwan[a]; Department of Mechanical Engineering, Chang Gung University, Kwei-Shan, Tao-Yuan, Taiwan[b]; Department of Periodontics, Division of Dentistry, Chang Gung Memorial Hospital, Kwei-Shan, Tao-Yuan, Taiwan[c]; Graduate Institute of Medical Mechatronics, Chang Gung University, Kwei-Shan, Tao-Yuan, Taiwan[d]; Department of Physiology and Pharmacology, Chang Gung University, Kwei-Shan, Tao-Yuan, Taiwan[e]

Guided tissue regeneration (GTR) therapy has been widely used to regenerate lost periodontium from periodontal disease. However, in terms of regenerative periodontal therapy, a multidrug-loaded biodegradable carrier can be even more promising in dealing with periodontal disease. In the current study, we fabricated biodegradable nanofibrous collagen membranes that were loaded with amoxicillin, metronidazole, and lidocaine by an electrospinning technique. The *in vitro* release behavior and the cytotoxicity of the membranes were investigated. A four-wall intrabony defect was created in rabbits for *in vivo* release analysis. The bioactivity of the released antibiotics was also examined. The experimental results showed that the drug-loaded collagen membranes could provide sustainable release of effective amoxicillin, metronidazole, and lidocaine for 28, 56, and 8 days, respectively, *in vivo*. Furthermore, the bioactivity of the released antibiotics remained high, with average bioactivities of 50.5% for amoxicillin against *Staphylococcus aureus* and 58.6% for metronidazole against *Escherichia coli*. The biodegradable nanofibrous multipharmaceutical membranes developed in this study may provide a promising solution for regenerative periodontal therapy.

Guided tissue regeneration (GTR) therapy has been widely used to regenerate lost periodontium resulting from periodontal disease. It has also been implemented in endodontic surgeries as a concomitant treatment during management of the endodontic-periodontal lesions (1–7). The function of GTR is to place a barrier membrane over the denuded root surfaces and the debrided periodontal defect to exclude epithelial growth and to allow specifically periodontal ligament and alveolar bone cells to repopulate the isolated space (8, 9). On the other hand, the amount of regenerated tissue is limited by the available space under the membrane; thus, previous studies reporting that the space-providing and wound-stabilizing effects of the barrier membrane might substantially influence the healing process (10, 11). In recent studies, biodegradable collagen membranes, both synthetic and natural, either used alone or in conjunction with different filler materials, have been recommended by several authors for use in the GTR process (12). The biodegradable collagen membranes serve not only as a barrier but also as a contributor toward maintaining the bony defect site to a certain extent (13). Reduced alveolar ridge resorption and better bone fill effect are subsequently demonstrated in the animal and clinical investigations. In addition, bone regeneration has also been proven to be enhanced by *N*-methyl-2-pyrrolidone (NMP), which is used as a plasticizer for polylactide or polyglycolide membranes, by increasing the bioactivity and bioavailability of autogenous bone morphogenetic proteins (14, 15).

Periodontal disease, however, is a chronic inflammation of the periodontium, resulting from bacterial infection. The GTR processes with biodegradable collagen membranes deal with only the regeneration of the lost tissue; chronic inflammation is currently treated by surgical debridement and systemic antibiotic therapy. The concept of antibiotic-loaded biodegradable collagen membranes has been introduced. It has been suggested that the direct delivery of antibiotics to the infection site at a MIC should be a safer and more effective approach compared to previous methods (16–18). For example, directed antibiotic delivery is used to treat osteomyelitis, a prolonged inflammation of the bone that brings about destruction of bone tissues and vascular channels that is caused by pathogenic microorganisms (19, 20). Alternatively, the direct delivery of antibiotics is also beneficial for other purposes, such as for the bone defects resulting from periodontal disease. Higher concentrations of antibiotics can be given, compared to systemic administration, which usually involves excessive doses to achieve substantial local effects.

In terms of regenerative periodontal therapy, the goals are extensive debridement of the periodontal defect and predictable restoration of the original tissue. A multidrug-loaded biodegradable carrier can be even more promising in dealing with periodontal disease. The current study focuses on the release behavior of amoxicillin, metronidazole, and lidocaine from a poly[(D,L)-lactide-*co*-glycolide] (PLGA) nanofibrous collagen membrane. The *in vitro* release behavior and cytotoxicity of the nanofibrous membranes are examined. A four-wall intrabony defect was constructed for *in vivo* release behavior analysis. The bioactivity of the released antibiotics is also examined. The objective of our study

Received 8 March 2012 **Returned for modification** 28 June 2012
Accepted 25 August 2012
Published ahead of print 4 September 2012
Address correspondence to Shih-Jung Liu, shihjung@mail.cgu.edu.tw.

doi:10.1128/AAC.00506-12

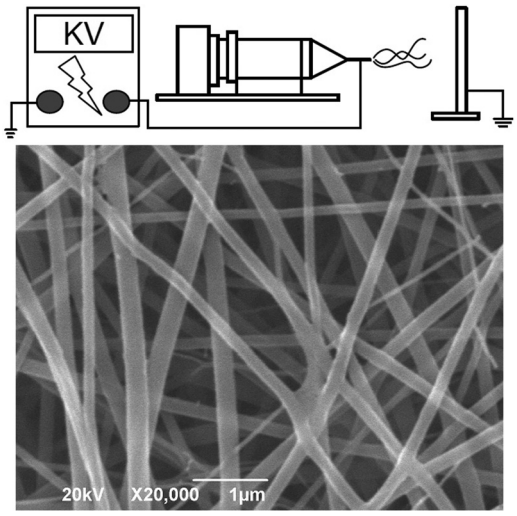

FIG 1 Schematic illustration of the electrospinning process equipment (top) and the morphology of the electrospun nanofibers observed with a scanning electron microscope (bottom).

is to develop a biodegradable, multipharmaceutical carrier to achieve prolonged drug release that would suppress periodontal bacterial growth and reduce the bioburden. In addition, the release behaviors of pharmaceutics are investigated in *in vitro* and *in vivo* experiments.

MATERIALS AND METHODS

Fabrication of the multipharmaceutical carrier. The poly[(D,L)-lactide-*co*-glycolide] (PLGA) used was commercially available material (Resomer RG 503; Boehringer, Germany) and had a lactide/glycolide ratio of 50:50 and an intrinsic viscosity of 0.4 dl/g. Collagen from bovine Achilles tendon, type I, and 1,1,1,3,3,3-hexafluoro-2-propanol (HFIP) were purchased from Sigma-Aldrich (St. Louis, MO). The drugs used included commercial-grade amoxicillin, metronidazole, and lidocaine hydrochloride (Sigma-Aldrich, St. Louis, MO).

The electrospinning setup utilized in this study consisted of a syringe and needle (internal diameter of 0.42 mm), a ground electrode, an aluminum sheet, and a high-voltage supply (21), as shown schematically in Fig. 1. The needle was connected to the high-voltage supply, which could generate positive direct current (DC) voltages and currents up to 35 kV and 4.16 mA/125 W, respectively. To prepare the membranes, PLGA and collagen (280 and 140 mg, respectively) were first dissolved in 1 ml of HFIP, while amoxicillin-metronidazole-lidocaine (35, 46, and 35 mg, respectively) was dissolved in 3 ml of HFIP. For electrospinning of nanofibrous membranes, 1 ml of the PLGA-collagen solution was delivered and electrospun by a syringe pump with a volumetric flow rate of 3.6 ml/h for the surface layer, followed by the electrospinning of 3 ml PLGA-amoxicillin-metronidazole-lidocaine solution with a volumetric flow rate of 1.2 ml/h for the core layer, and finally spinning another 1 ml of PLGA-collagen solution for the second surface layer. A three-layered membrane, with PLGA-collagen as the surface layers and PLGA-drugs at the core, was thus obtained. The thickness of the membrane was measured and found to be 0.116 mm.

The morphology of the electrospun nanofibers was observed on a scanning electron microscope (SEM) (Hitachi S-3000N; Hitachi, Japan) after gold coating. The diameters of the spun nanofibers shown in Fig. 1 ranged from 45 to 280 nm.

***In vitro* release behavior.** The release characteristics of amoxicillin, metronidazole, and lidocaine from the nanofibrous membranes were determined by the *in vitro* elution method. Samples with an area of 2 cm by 3 cm, cut from the electrospun membranes, were placed in glass test tubes (one sample per test tube, with a total of 3 test tubes) with 1 ml of phosphate buffer solution (0.15 mol/liter; pH 7.4). The glass test tubes were incubated at 37°C for 24 h before the eluent was collected and analyzed. Fresh phosphate buffer solution (1 ml) was then added for the next 24-hour period, and this procedure was repeated daily until the membrane was completely dissolved. The drug concentrations in the eluents were determined by the high-performance liquid chromatography (HPLC) assay standard curve.

Cytotoxicity of nanofibrous membranes. The cytotoxicity of the material was examined by the 3-(4,5-dimethylthiazol-2-yl)-2,5-diphenyltetrazolium bromide (MTT) assay (Roche, Germany) of cell viability. Electrospun multipharmaceutical nanofibers were cut out with a hole puncher and put into the wells of 24-well culture plates. Human fibroblasts obtained from the foreskins of patients (1 to 3 years of age) undergoing surgery were seeded (5×10^3 cells/well) in Dulbecco's modified Eagle's medium (DMEM) at 37°C under 5% CO_2-95% air conditions until cell confluence. Cell viability was monitored at 1, 3, 7, and 14 days by MTT assays and quantified using an enzyme-linked immunosorbent assay (ELISA) reader. In this study, pure PLGA membrane, multipharmaceutical PLGA membrane, and commercially available membrane (OsseoGuard resorbable collagen membrane OG3040 [30 mm by 40 mm], Collagen Matrix Inc., NJ) were compared with the control.

Model of four-wall intrabony defect. Six New Zealand White rabbits (age, 8 to 12 weeks; average weight, 1.5 kg) were used for animal testing. A four-wall intrabony defect was created on the right tibia bone of each rabbit. All surgical procedures and protocols for care after surgery were performed according to our facility's guidelines for the care and use of laboratory animals under the supervision of a licensed veterinarian.

After the rabbits were sedated, they were prepared for surgery. The surgical site was depilated, washed with soft soap and ethanol directly before surgery, and disinfected with 70% ethanol. The posterior part of the animals was covered with a sterile blanket. An incision was made on the proximal-anterior part of the tibia, penetrating the epidermis, dermis, and the fascias. An additional medial-anterior incision was made through the periosteum, which was elevated by a self-retaining retractor. A 5-mm by 20-mm bone defect was prepared by using a 2.5-mm-diameter twist drill (Medicon CMS, Tuttlingen, Germany). The bone defect penetrated well into the marrow space. Copious irrigation of physiological saline solution was used during the preparation to prevent overheating. The biodegradable membrane was then placed on the bone defect (Fig. 2). After the whole procedure was completed, the soft tissue was repositioned and sutured, and the superficial layers were closed with vertical mattress intracutaneous sutures. After surgery, all animals were monitored for pain and distress as appropriate for the condition and degree of invasiveness. The staff at the animal center assessed the presence or absence of pain or distress and gave the animals the adequate analgesics during the study period.

***In vivo* release behavior.** Intralesion (from skin to the bone defect site) aspiration with a 19-gauge needle was performed on days 1, 2, 4, 7, 14, 21, 28, 35, 42, 49, and 56 for *in vivo* release analysis. The antibiotics and lidocaine concentrations of the tapped fluid were determined by an HPLC assay. The HPLC analyses were conducted on a Hitachi L-2200 multisolvent delivery system. All tapping samples were assayed after dilution with phosphate-buffered saline and were assessed according to the assay standard curve. A calibration curve was made for each set of the measurements (correlation coefficient of >0.99).

Bioactivity of released antibiotics. The bioactivity of the released amoxicillin on *Staphylococcus aureus* (ATCC 65389) was determined by using an antibiotic disk diffusion method in nutrient broth (beef extract, peptone; Difco Laboratories). Eight microliters of solution from each daily buffer sample was pipetted on 6-mm disks. The disks were placed on nutrient agar plates (beef extract, peptone, agar; Difco Laboratories) and seeded with a layer of *Staphylococcus aureus*, and the zones of inhibition were measured with a micrometer after 16 to 18 h of incubation at 35°C. A

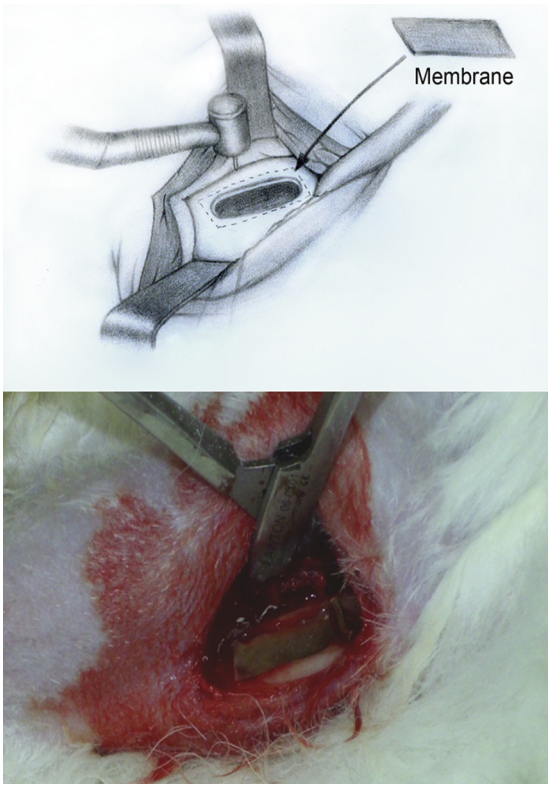

FIG 2 Sketch of the four-wall intrabony defect created (top) and surgical photograph (bottom) of the defect used in the *in vivo* analysis.

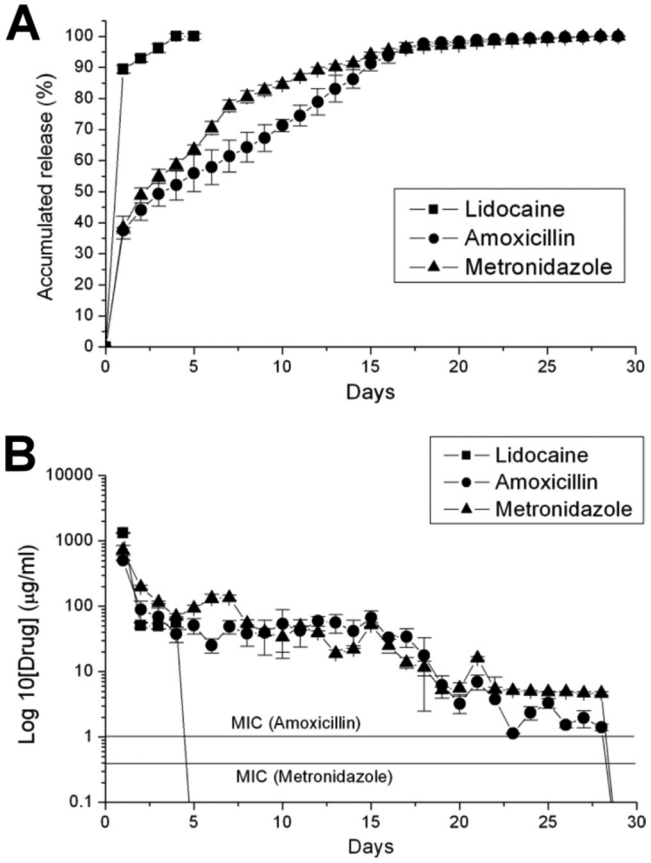

FIG 3 (A) *In vitro* accumulated release curves of amoxicillin, metronidazole, and lidocaine from a PLGA nanofibrous membrane. (B) *In vitro* daily concentration curves of amoxicillin, metronidazole, and lidocaine from a PLGA nanofibrous membrane.

calibration curve was first determined by six different standard concentrations (0.01, 0.1, 1, 10, 100, and 1,000 mg/ml). The released concentration of amoxicillin was then determined by interpreting the curve. The bioactivities of the incubated amoxicillin on *Staphylococcus aureus* (ATCC 65389) were determined by the following equation: Bioactivity (%) = diameter of the sample inhibition zone/diameter of the maximum inhibition zone.

The bioactivity of metronidazole was performed with the same scheme against *Escherichia coli* (ATCC 25922).

The MIC of amoxicillin on *Staphylococcus aureus* (ATCC 65389) was determined using an antibiotic tube dilution method in cation-supplemented Mueller-Hinton broth (Difco Laboratories). Amoxicillin was diluted serially 2-fold in tubes containing 0.5 ml of the cation-supplemented Mueller-Hinton broth. The MIC of metronidazole to *Escherichia coli* (ATCC 25922) was also determined by the same method. The MIC of amoxicillin against *Staphylococcus aureus* was determined to be 1 μg/ml, while the MIC of metronidazole against *Escherichia coli* was determined to be 0.4 μg/ml (22).

RESULTS

Figure 3 displays the *in vitro* accumulated release curves and HPLC concentration curves of amoxicillin, metronidazole, and lidocaine from a PLGA nanofibrous membrane. In Fig. 3A, a burst release behavior in the beginning stage was noted from all three pharmaceuticals. In this stage, lidocaine exhibited the fastest and greatest amount of release. In the second stage, metronidazole exhibited a more rapid release rate compared to the release rates of amoxicillin and lidocaine. In the last stage, the release curves were flat and smooth in all three pharmaceuticals. In Fig. 3B, all lidocaine was released by the 5th day after elution. The desired concentrations of amoxicillin and metronidazole were attained on the 28th day, even though the biodegradable membrane was entirely dissolved on the same day. The concentrations of all the antibiotics were above the levels of MIC during the whole *in vitro* release behavior analysis.

Figure 4 shows the results of cytotoxicity tests from the MTT assays of cell viability. In the study, pure PLGA membrane, multipharmaceutical PLGA membrane, and commercially available OG membrane were compared with the control. All membranes studied showed no signs of cytotoxicity from day 1 to day 14. In the multipharmaceutical membrane (PLGA plus drugs) group, cell viability showed little decrease compared to the cell viabilities of other groups on the first day and 3rd day after the surgery, but no significant difference was found.

Figure 5 shows the *in vivo* HPLC concentration curves of amoxicillin, metronidazole, and lidocaine from a PLGA nanofibrous membrane. From the results, the concentrations of lidocaine and amoxicillin could not be obtained on the 14th and 35th day, respectively, after surgery. The concentration of metronidazole was still available on the 56th day after the operation. The concentrations of all antibiotics were above the MIC level during the whole *in vivo* release analysis.

Figure 6 displays the *in vivo* concentration and bioactivity curves of amoxicillin and metronidazole. In Fig. 6A, the average bioactivity of amoxicillin against *Staphylococcus aureus* was 50.5%

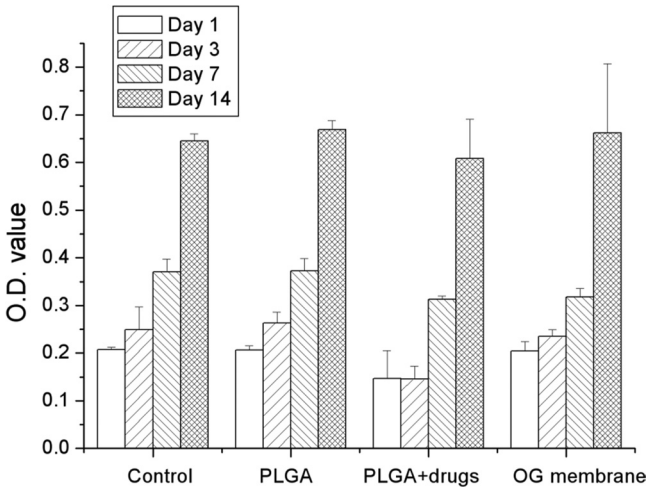

FIG 4 Cytotoxicity tests from MTT assays of cell viability. O.D., optical density.

during the whole experiment. In Fig. 6B, the average bioactivity of metronidazole against *Escherichia coli* was 58.6%.

DISCUSSION

Antibiotic-loaded carriers (23), which are made of biodegradable polymeric membranes, have several advantages. First, biodegradable membranes provide bactericidal concentrations of antibiotics for the prolonged time needed to completely treat the particular infection. Second, variable biodegradability from weeks to months may allow many types of infections to be treated. Third, the biodegradable membranes dissolve, thus eliminating the need for removal. Last, because the biodegradable membranes dissolve slowly, the soft tissue or bone defect will slowly fill with tissue, thus no longer requiring reconstruction. Elsner et al. (24, 25) fabricated antibiotic-eluting composite fibers, which consisted of a polyglyconate core and a porous poly[(D,L)-lactide-*co*-glycolide] shell, for use as basic dressing elements, by freeze-drying inverted emulsions. The results demonstrated the ability of the fibers to accelerate wound healing compared to an unloaded form of the material

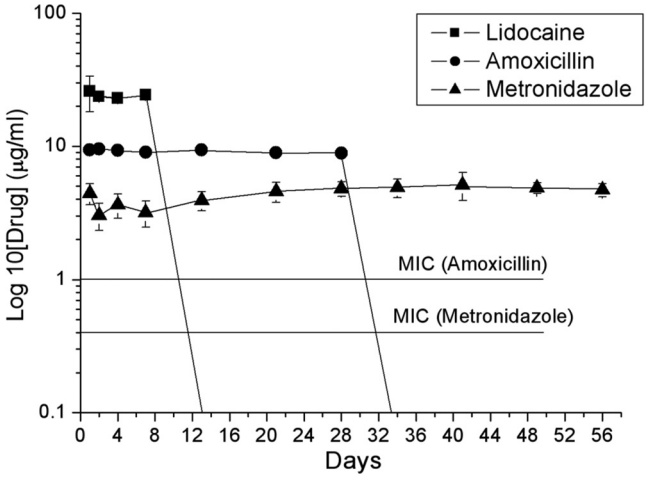

FIG 5 *In vivo* HPLC concentration curves of amoxicillin, metronidazole, and lidocaine from a PLGA nanofibrous membrane.

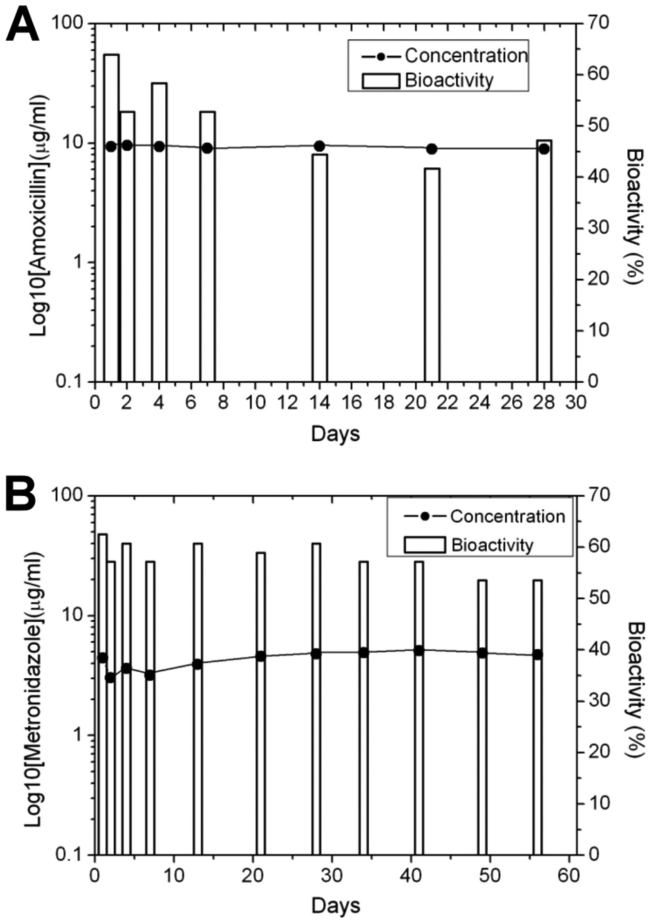

FIG 6 *In vivo* concentration and bioactivity curves of amoxicillin (A) and metronidazole (B).

and a nonadherent dressing material. Teo et al. (26) developed 3-dimensional polycaprolactone-tricalcium phosphate mesh for the delivery of gentamicin sulfate to infected wounds. The *in vitro* and *in vivo* results showed efficient elimination of bacteria within 2 h and low cytotoxicity. Previous studies, however, focused on the effect of released antibiotics from the biodegradable carrier by using the soft tissue defect model. Discussions of those effects on the bone defect model are limited.

In the current study, we demonstrate the release ability of a multipharmaceutical carrier based on a biodegradable collagen-PLGA membrane on the bony defect model. The different release behaviors of pharmaceuticals are shown in the *in vitro* and *in vivo* investigations. From the results of the MTT assays of cell viability (Fig. 4), the novel multipharmaceutical carrier shows comparable biocompatibility with the control and commercialized product. Despite the fact that PLGA in the nanofibrous matrices can be hydrolyzed in aqueous solution and releases lactic acid, the results of the cell viability did not show any significant variations during the experiment. The possible influence of released acid on cell proliferation is negligible. The initial lower cell viability (1st day and 3rd day), which has no significant difference compared to other membranes at the same time, should be a result of the burst release of pharmaceuticals in the early stage. Furthermore, the concentration of the antibiotics is over the level of MIC in the *in*

vitro investigation (Fig. 3B), and the average bioactivity of the antibiotics is over 50% in the *in vivo* investigation (Fig. 6). It should be noted that a membrane size (2 cm by 3 cm) commonly used clinically for periodontal treatment was adopted for the *in vitro* test. The daily concentrations obtained are completely dependent upon the size of the membrane selected and the volume of the fluid vehicle. A 2-cm by 3-cm membrane in 1 ml of fluid may or may not be a valid biologic test. The accumulated drug release should be considered a more valid calculation. The results suggest that the released antibiotics from the novel multipharmaceutical carrier are capable of treating chronic inflammation from periodontal disease.

It is generally believed that the release mechanisms are controlled by channel diffusion, osmotic pressure, and then polymer degradation (27). In the first stage, the release behavior is controlled by the effects of channel diffusion, i.e., imperfectly dissolved substances of pharmaceuticals in the nanofibrous matrix are transported from an area of higher concentration to an area of lower concentration by means of concentration gradients. This phenomenon is confirmed by the initial burst release behavior of all pharmaceuticals in the *in vitro* release behavior analysis (Fig. 3A). All pharmaceuticals used in this study are water soluble; however, the octanol-water ratios (log P) (DrugBank database [http://www.drugbank.ca/]) of amoxicillin, metronidazole, and lidocaine are 0.87, 0.02, and 2.44, respectively. Lidocaine exhibits a relatively not water-soluble characteristic compared to the other two antibiotics in the study, exhibiting the fastest and greatest amount of release in the first stage. In the second stage, the release of antibiotics is controlled by the effects of osmotic pressure. In this stage, the dissolving substances of the pharmaceuticals separate out from the nanofibrous matrix by means of hydrostatic pressure. Theoretically, substances with smaller molecular weights exhibit more rapid release rates than those with larger molecular weights. In this study, the molecular weights of amoxicillin, metronidazole, and lidocaine are 365.41, 171.16, and 234.34, respectively (DrugBank database [http://www.drugbank.ca/]). In the accumulated release curves shown in Fig. 3A, metronidazole exhibits a faster release rate than other pharmaceuticals do in the second stage. In the third stage, the release of antibiotics is mainly dependent on the effects of polymer degradation. In this study, the accumulated release curves of the three pharmaceuticals are flat and smooth. The expected secondary burst release behavior (28), which results from degradation of polymeric carrier, is not seen. This may be due to the PLGA membranes providing a more even degradation behavior than the disk-shape biodegradable carrier can provide, which was discussed in the previous study (28).

In the animal testing, a bony defect was created on the tibia of rabbits (Fig. 2) to mimic a four-wall intrabony defect, which results from an extraction socket. In this study, the HPLC concentration curves of amoxicillin, metronidazole, and lidocaine show different pictures in the *in vitro* (Fig. 3B) and *in vivo* (Fig. 5) investigations. In the *in vitro* investigation, lidocaine showed total liberation on the 5th day, and the concentrations of amoxicillin and metronidazole were still obtainable on the 28th day. In the *in vivo* investigation, however, the concentrations of lidocaine and amoxicillin were not obtainable on the 14th and 35th day, respectively, and the concentration of metronidazole was still available on the 56th day after the operation. For all pharmaceuticals, the *in vivo* environment seems to provide a slower metabolic rate than the *in vitro* environment provides. This might explain why the total period of *in vivo* drug release is longer than that of the *in vitro* drug release. In addition, lidocaine is a relatively low water-soluble drug compared to the other two antibiotics, thus exhibiting the fastest release rate and the shortest total release period. It is interesting to note that the drug release period of metronidazole is nearly twice as long as that of amoxicillin in the *in vivo* investigation. According to the pharmacodynamics (DrugBank database [http://www.drugbank.ca/]), amoxicillin exhibits approximately 20% protein-bound form in blood serum, and its half-life is only 61.3 min. In the *in vivo* investigation, by using the technique of HPLC assay, the concentration of amoxicillin may be underestimated.

Conclusions. GTR therapy has been widely used to regenerate lost periodontium due to periodontal disease. In terms of regenerative periodontal therapy, however, a multidrug-loaded biodegradable carrier can be even more promising in dealing with periodontal disease. We have fabricated amoxicillin, metronidazole, and lidocaine-loaded biodegradable nanofibrous collagen membranes and investigated the *in vitro* and *in vivo* release behavior of these pharmaceuticals from the membranes. The biodegradable multipharmaceutical carrier shows its ability to achieve prolonged drug release and effective bioactivity in the *in vitro* and *in vivo* investigations. The biodegradable multipharmaceutical carrier developed in this study may provide a promising strategy for regenerative periodontal therapy.

REFERENCES

1. **Carmagnola D, Adriaens P, Berglundh T.** 2003. Healing of human extraction sockets filled with Bio-Oss. Clin. Oral Implants Res. **14**:137–143.
2. **LeGeros RZ, Parsons JR, Daculsi G, Driessens F, Lee D, Liu ST, Metsger S, Peterson D, Walker M.** 1988. Significance of the porosity and physical chemistry of calcium phosphate ceramics. Biodegradation–bioresorption. Ann. New York Acad. Sci. **523**:268–271.
3. **Neiva RF, Tsao YP, Eber R, Shotwell J, Billy E, Wang HL.** 2008. Effects of a putty-form hydroxyapatite matrix combined with the synthetic cell-binding peptide P-15 on alveolar ridge preservation. J. Periodontol. **79**: 291–299.
4. **Serino G, Biancu S, Iezzi G, Piattelli A.** 2003. Ridge preservation following tooth extraction using a polylactide and polyglycolide sponge as space filler: a clinical and histological study in humans. Clin. Oral Implants Res. **14**:651–658.
5. **Serino G, Rao W, Iezzi G, Piattelli A.** 2008. Polylactide and polyglycolide sponge used in human extraction sockets: bone formation following 3 months after its application. Clin. Oral Implants Res. **19**:26–31.
6. **Stanley HR, Hall MB, Clark AE, King CJ, III, Hench LL, Berte JJ.** 1997. Using 45S5 bioglass cones as endosseous ridge maintenance implants to prevent alveolar ridge resorption: a 5-year evaluation. Int. J. Oral Maxillofac. Implants **12**:95–105.
7. **Zitzmann NU, Schärer P, Marinello CP, Schüpbach P, Berglundh T.** 2001. Alveolar ridge augmentation with Bio-Oss: a histologic study in humans. Int. J. Periodont. Restor. Dent. **21**:288–295.
8. **Gottlow J, Nyman S, Karring T, Lindhe J.** 1984. New attachment formation as a result of controlled tissue regeneration. J. Clin. Periodontol. **11**:494–503.
9. **Nyman S, Gottlow J, Karring T, Lindhe J.** 1982. The regenerative potential of the periodontal ligament. An experimental study in the monkey. J. Clin. Periodontol. **9**:257–265.
10. **Haney JM, Nilvéus RE, McMillan PJ, Wikesjo UME.** 1993. Periodontal repair in dogs: expanded polytetrafluoroethylene barrier membranes support wound stabilization and enhance bone regeneration. J. Periodontol. **64**:833–890.
11. **Wikesjo UME, Nilvéus R.** 1990. Periodontal repair in dogs: effect of wound stabilization on healing. J. Periodontol. **61**:719–724.
12. **McAllister BS, Haghighat K.** 2007. Bone augmentation techniques. J. Periodontol. **78**:377–396.

13. **Chen ST, Darby IB, Reynolds EC.** 2007. A prospective clinical study of non-submerged immediate implants. Clinical outcomes and esthetic results. Clin. Oral Implants Res. **18**:552–562.
14. **Miguel BS, Ghayor C, Ehrbar M, Jung RE, Zwahlen RA, Hortschansky P, Schmoekel HG, Weber FE.** 2009. *N*-methyl pyrrolidone as a potent bone morphogenetic protein enhancer for bone tissue regeneration. Tissue Eng. Part A **15**:2955–2963.
15. **Weber FE, San Miguel B, Ehrbar M, Ghayor C, Jung R, Zwahlen R.** 2006. The small molecule NMP is an enhancer of bone regeneration. Bone **38**:S20–S21.
16. **Cornell CN, Tyndall D, Waller S, Lane JM, Brause BD.** 1993. Treatment of experimental osteomyelitis with antibiotic-impregnated bone graft substitute. J. Orthop. Res. **11**(5):619–626.
17. **Ragel CV, Vallet-Regi M.** 2000. In vitro bioactivity and gentamicin release from glass polymer-antibiotic composites. J. Biomed. Mater. Res. **51**(3):424–429.
18. **Shinto Y, Uchida A, Korkusuz F, Araki N, Ono K.** 1992. Calcium hydroxyapatite ceramic used as a delivery system for antibiotics. J. Bone Joint Surg. Br. **74**(4):600–604.
19. **Garvin K, Feschuk C.** 2005. Polylactide-polyglycolide antibiotic implants. Clin. Orthop. Relat. Res. **437**:105–110.
20. **Lazzarini L, Mader JT, Calhoun JH.** 2004. Osteomyelitis in long bones. J. Bone Joint Surg. Am. **86-A**(10):2305–2318.
21. **Liu SJ, Kau YC, Chou CY, Chen JK, Wu RC, Yeh WL.** 2010. Electrospun PLGA/collagen nanofibrous membrane as early-stage wound dressing. J. Membr. Sci. **355**:53–59.
22. **Wu H, Shi XD, Wang HT, Liu JX.** 2000. Resistance of Helicobacter pylori to metronidazole, tetracycline and amoxycillin. J. Antimicrob. Chemother. **46**:121–123.
23. **Zilberman M, Elsner JJ.** 2008. Antibiotic-eluting medical devices for various applications. J. Contr. Release **130**:202–215.
24. **Elsner JJ, Egozi D, Ullmann Y, Berdicevsky I, Shefy-Peleg A, Zilberman M.** 2011. Novel biodegradable composite wound dressings with controlled release of antibiotics: results in guinea pig burn model. Burns **37**:896–904.
25. **Elsner JJ, Zilberman M.** 2009. Antibiotic-eluting bioresorbable composite fibers for wound healing applications: microstructures, drug delivery and mechanical properties. Acta Biomater. **5**:2872–2883.
26. **Teo EY, Ong SY, Chong MS, Zhang Z, Lu J, Moochhala S, Ho B, Teoh SH.** 2011. Polycaprolactone-based fused deposition modeled mesh for delivery of antibacterial agents to infected wounds. Biomaterials **32**:279–287.
27. **Seigel RA, Langer R.** 1990. Mechanistic studies of macromolecular drug release from macroporous polymers. II. Models for the kinetics of drug release. J. Contr. Release **14**:153–167.
28. **Lee FY, Chen DW, Hu CC, Hsieh YT, Liu SJ, Chan EC.** 2011. In vitro and in vivo investigation of drug-eluting implants for the treatment of periodontal disease. AAPS PharmSciTech. **12**:1110–1115.